ABSTRACT

NGUYEN, ALAN DINH. Modeling Glutathione Dynamics in Response to Chemical Perturbation Suggests the Importance of Cysteine Upregulationin Hepatocyte Function

Glutathione (GSH) is a tripeptide present in the cells of animals, plants, and fungi and plays an important role in preventing damage to the cell from stressors such as drugs, toxins, heavy metals, and reactive oxygen species (ROS). GSH is normally present in cells at 500 to 10,000μM, but the concentration can drop considerably when protecting the cell from a source of stress. Chronic deficiencies in GSH have been implicated in various diseases such as cancer, diabetes, neurodegeneration, cardiovascular disease, and more. The purpose of this study was to develop a mathematical model of GSH dynamics in liver cells and further define potential feedback mechanisms of regulation. To provide a basis with which to evaluate the model, Carbon-13 Nuclear Magnetic Resonance (^{13}C NMR) imaging was used to monitor JM1 rat hepatoma cells exposed to monobromobimane (mBBr), which conjugates GSH and is subsequently removed from the cell. Data from this experimental work was then used to estimate relevant parameters and evaluate overall model accuracy. In addition, two different feedback mechanisms, one through the amino acid cysteine and the second through γ-glutamyl-L-cysteine, were explored for possible regulation of GSH behavior in response to mBBR exposure. Results from this work suggests that the model represents realistic biological mechanisms, being able to accurately replicate experimental data. Furthermore, it is demonstrated that, of the two feedback mechanisms, the upregulation of cysteine when glutathione levels are low has a much more profound effect on the recovery of normal intracellular glutathione concentrations.

Modeling Glutathione Dynamics in Response to Chemical Perturbation Suggests the Importance of Cysteine Upregulationin Hepatocyte Function

by
Alan Dinh Nguyen

A thesis submitted to the Graduate Faculty of
North Carolina State University
in partial fulfillment of the
requirements for the degree of
Master of Science

Biomedical Engineering

Raleigh, North Carolina

2016

APPROVED BY:

_____	_____
Shawn Gomez Committee Chair	Jeffrey Macdonald
_____	
Michael Gamcsik	

BIOGRAPHY

In 2009, I obtained my bachelor's degree in biomedical engineering at Case Western Reserve University and began work at a startup company whose product was an autologous stem cell treatment for stroke, critical limb ischemia, and certain forms of cancer. In 2011, I married the light of my life. In 2013, I enrolled in the joint biomedical engineering master's degree program at North Carolina State University and University of North Carolina at Chapel Hill, partially because the 5-year time limit on my MCAT scores from 2008 was about to expire. In 2014, the startup went out of business--as startups are wont to do--and I transitioned to the nightshift at a large medical device company. In 2015, my son was born, and now I was a father who studied during the day and sat down for dinner and reading aloud before heading to work at night. In 2016, I did the final proofreading of this paper sitting on a bench, looking up to wave at my wife and son as they rode the slow-moving miniature train around the perimeter of Pullen Park.

TABLE OF CONTENTS

LIST OF FIGURES

LIST OF ABBREVIATIONS

GSH	Glutathione
ROS	Reactive oxygen species
mBBr	Monobromobimane
GSBi	Glutathione-bimane conjugate
ATP	Adenosine triphosphate
NADH	Nicotinamide adenine dinucleotide
$FADH_2$	Flavin adenine dinucleotide
H_2O_2	Hydrogenperoxide
GSSG	Glutathionedisulfide
GCL	Glutamate-cysteineligase
GCLC	Glutamate-cysteine ligase catalyticsubunit
GCLM	Glutamate-cysteine ligase modifier subunit
GS	Glutathione synthase
NMR	Nuclear magnetic resonance
DMSO	Dimethyl sulfoxide
GluCys	Gamma-glutamyl-cysteine

CHAPTER 1

Introduction

The cellular processes of the human body are tightly regulated based on innumerable checks and balances that ensure proper levels of nutrients and removal of toxins so that each cell can perform their specialized functions. For every question that advancements in science answer, more unknowns present themselves. The regulation of reactive oxygen species by antioxidants has been the subject of research since the 19th century, though it was focused on industrial processes to prevent metal corrosion and vulcanizing rubber, when antioxidant strictly referred to a chemical that prevented the consumption of oxygen [48]. Research on antioxidants and regulation of oxidants in human biology is somewhat newer, having been revolutionized by the discovery of Vitamins A, C, and E in the early half of the 20th century [48]. Glutathione is one such antioxidant present in human cells, and it plays an important role in maintaining normal intracellular conditions. This thesis aims to provide a robust mathematical model of the cellular pathways involved in glutathione's regulation of reactive oxygen species in human cells.

1.1 Overview of Reactive Oxygen Species

ROS refers to chemically reactive molecules and free radicals containing oxygen and are a natural byproduct of normal metabolism of oxygen [1]. Since the mid-20th century,

thousands of research articles have indicated that reactive oxygen species (ROS) are detrimental to human health, playing a role in disease states such as cancer, diabetes, neurodegeneration, cardiovascular diseases, and aging. On the other hand, ROS have also been demonstrated as necessary parts of immune defense, antibacterial action, and signal transduction [2]. It can therefore be concluded that a proper homeostasis of ROS is a vital part of maintaining human health.

Aerobic organisms such as humans use oxygen molecules in the process of aerobic energy metabolism which produces adenosine triphosphate (ATP), an important, high-energy molecule used in intracellular energy transfer [3].

Glycolysis is a metabolic pathway that converts glucose ($C_6H_{12}O_6$, a simple sugar largely synthesized in the body from the consumption of protein, fats, and carbohydrates) into pyruvate ($CH_3COCOOH$). Pyruvate dehydrogenase complex, a complex of three enzymes (pyruvate dehydrogenase, dihydrolipoyltransacetylase, and dihydrolipoyl dehydrogenase), interact with pyruvate to form the molecule acetyl coenzyme A (acetyl-CoA, $C_{23}H_{38}N_7O_{17}P_3S$). Acetyl-CoA is used in many biochemical reactions, but with reference to aerobic energy metabolism, acetyl-CoA is an input to the citric acid cycle (also called the tricarboxylic acid cycle [TCA Cycle] and the Krebs Cycle) within the mitochondria of the cell. Figure 1.1 provides an overview of the cycle.

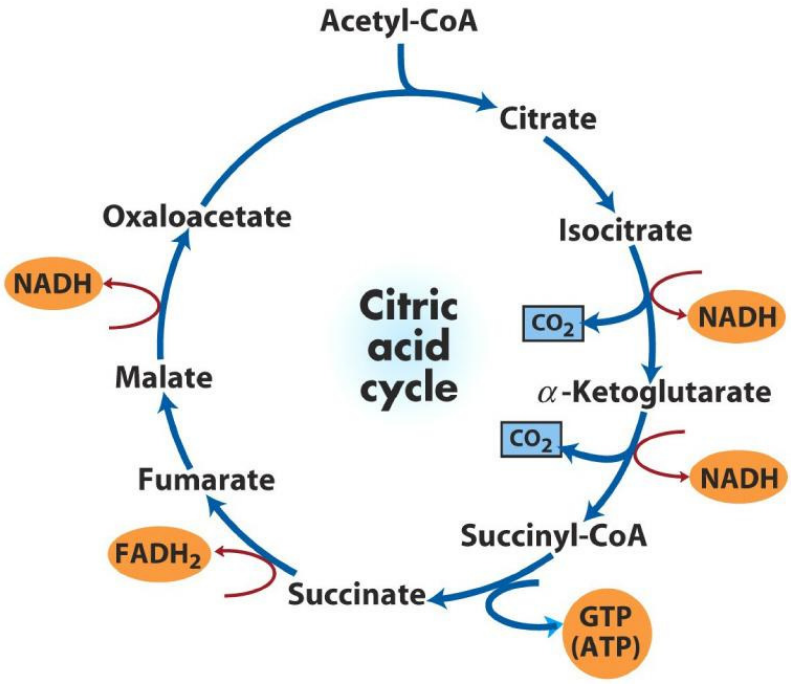

Figure 1.1. The Citric Acid Cycle. Outputs are shown as branching off of the main cycle's pathway. Abbreviations are as follows: Acetyl-CoA, Acetyl Coenzyme A; NADH, Nicotinamide Adenine Dinucleotide; GTP, Guanosine Triphosphate; ATP, Adenosine Triphosphate; $FADH_2$, Flavin Adenine Dinucleotide; CO_2, Carbon Dioxide. [44].

The citric acid cycle begins with the reaction between a two-carbon acetyl group from acetyl-CoA and a four-carbon oxaloacetate ($C_4H_4O_5$, created from previous iterations of the citric acid cycle and the breakdown of citrate) that forms the six-carbon compound citrate ($C_6H_5O_7^{3-}$). Citrate then undergoes a series of chemical reactions and outputs: a regenerated oxaloacetate, an energy-rich nicotinamide adenine dinucleotide (NADH), and flavin adenine dinucleotide ($FADH_2$) [4]. NADH and $FADH_2$ are now precursors to the major metabolic pathway for energy, oxidative phosphorylation.

Oxidative phosphorylation is the process by which the mitochondria create the bulk of the ATP used by most aerobic organisms. The NADH and $FADH_2$ from the citric acid cycle react with a series of enzymes within the membrane of the mitochondria that make up a subprocess called the electron transport chain. The electron transport chain gradually oxidizes NADH and $FADH_2$, removing electrons (thereby converting them to NAD^+ and FAD) and ultimately passing the electrons to oxygen molecules. With each removal of a negatively charged electron within the mitochondrial membrane, positively charged protons within solution are drawn and arranged to form a proton gradient across the inner mitochondrial membrane [5]. This process can be seen in Figure 1.2.

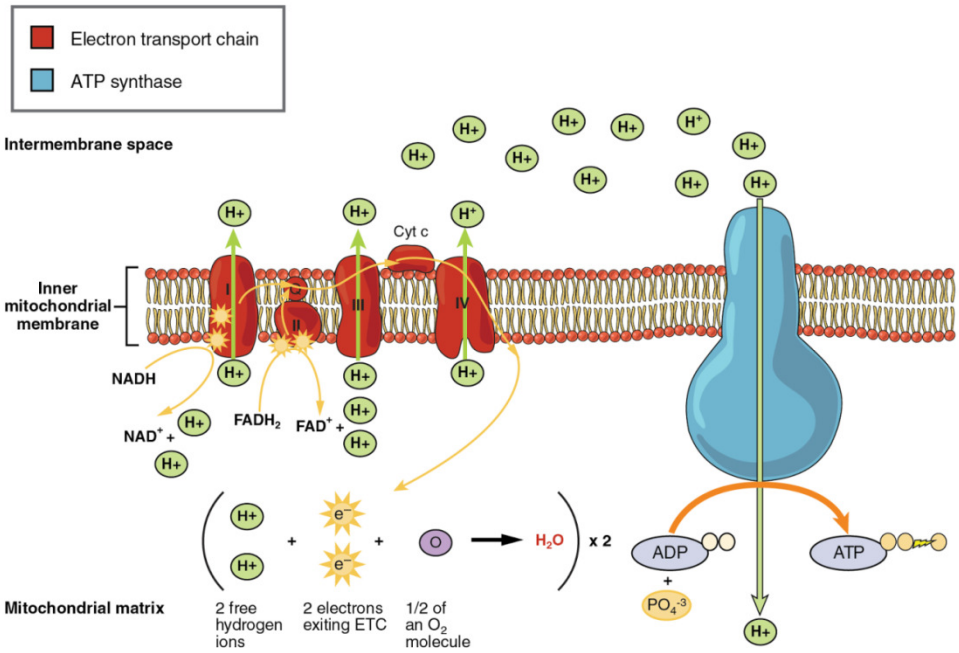

Figure 1.2. The Electron Transport Chain. Removal of negative eletrons allows positively charged protons (H^+) to form a gradient across mitochondrial membrane. Proton flow catalyzes ATP synthesis. [45]

The gradient causes protons to flow back through the membrane, interacting with the enzyme ATP synthase, causing a conformational change that catalyzes ATP synthesis [6]. This movement can be likened to a dam using the flow of water through a turbine to generate power.

However, the important step relevant to this thesis is the contribution of electrons from NADH and $FADH_2$ to oxygen during the oxidative phosphorylation step. When oxygen receives electrons during this step and other electron transfer reactions in the body, it has the potential to prematurely and incompletely reduce to produce highly reactive oxygen molecules such as superoxides (when there is a single unpaired electron in O_2's electron orbit causing a net negative charge of -1), hydrogen peroxide (H_2O_2), and hydroxyl radicals (OH with an unpaired electron on the oxygen atom). Some studies estimate that 0.2% to 2% of O_2 consumed by mitochondria generates superoxides [7,8].

A number of detrimental effects have been linked to interactions with ROS. Superoxides (O_2^-) can react with nitric oxide (NO) to form peroxynitrite ($ONOO_2^-$) within mitochondria, which has been shown to cause damage to DNA through strand breakage and causes subsequent cell necrosis, apoptosis, and carcinogenesis and contributes to diabetes, stroke, and neurodegenerative disorders [9,10,11].

Fortunately, there are a number of antioxidant enzyme systems that scavenge ROS when they are generated. Superoxide dismutase is an important class of enzymes that can render superoxides to hydrogen peroxide (H_2O_2), which is then reduced to water by the enzyme catalase and glutathione (GSH; $C_{10}H_{17}N_3O_6S$) [12].

1.2 The Problem

GSH is a tripeptide composed of three amino acids--glutamate, cysteine, and glycine, (γ-L-glutamyl-L-cysteinyl-glycine)-- and is present at 0.5 - 10 mM in mammalian cells and 2 - 20 μM in plasma, which is considered a relatively high concentration [46]. The cysteine residue readily oxidizes to the form glutathione disulfide (GSSG; $C_{20}H_{32}N_6O_{12}S_2$) when it detoxifies free radicals and ROS and then is effluxed from the cells. GSH is synthesized from its respective amino acids (cysteine, glycine, and glutamate) catalyzed by glutamate-cysteine ligase (GCL) and GSH synthetase. It has been shown that GSH synthesis is primarily regulated by GCL activity, cysteine availability, and GSH feedback inhibition [13].

The bioavailability of cysteine and its oxidized form cystine is known to be the rate limiting step for GSH synthesis. Sodium dependent and independent transporters convey cystine into the cell for synthesis [15]. Cellular stress promotes cystine uptake and increases synthesis of a molecule called gamma-glutamyl-cysteine, which increases GSH synthesis. This process then self-regulates and leads to inhibition of GSH via negative feedback [16].

GSH plays a role in protecting the cell from a myriad of stressors. It is vital in detoxifying electrophiles, maintaining thiol status of proteins, maintaining a reservoir of cysteine, nitric oxide homeostasis, modulating protein activity, assisting in DNA synthesis and immune function [46]. Conversely, cancer cells exhibiting high concentrations of GSH are more resistant to chemotherapeutic drugs, and GSH-depletion techniques have been used to increase cancer cell susceptibility [47].

With GSH being such a key player in a myriad of applications, it is important to understand how GSH levels affect and are affected by cellular stresses. The intention of this paper is to provide a mathematical model that illustrates GSH depletion by the application of cellular stress, removal of the stressor, and GSH resynthesis from its constituent parts through increased cellular demand.

1.3 The Purpose

GSH plays an important role in balancing the removal of ROS versus the generation of ROS, as finely tuned ROS levels are a necessary part of human health. A lack of ROS generating species has been implicated as key factors in immunodeficiency related to recurrent infections such as pneumonia, abscesses, and osteomyelitis [17]; hormone production via the thyroid [18]; and cellular aging [19,20]. Additionally, as previously mentioned, an excess of ROS can inflict DNA damage to initiate or progress carcinogenesis via ROS-dependent base modifications, rearrangement, miscoding, and activation of oncogenes [21]; cardiovascular disease via hypertension [22]; and neurological diseases such as Alzheimer's disease and Parkinson's disease via neurotoxicity and neurodegeneration [23, 24]. Needless to say, aging, cancer (22.5% of deaths), cardiovascular disease (23.5% of deaths), and neurological disease (3.3% and 1.0% of deaths for Alzheimer's and Parkinson's diseases, respectively) are among the leading causes of death and loss of quality of life in the United States [25]. While each issue is in it of itself a complex web of biochemistry, genetics, environmental factors, diet, and more, being able to understand and predict how

GSH weaves into the dynamics and responds to external stimuli will provide greater insight into pathogenesis and treatment.

CHAPTER 2

Biochemistry of Glutathione

GSH is formed from its constituent amino acids, glutamate and cysteine, via the following two steps:

1. L-glutamate + L-cysteine + ATP → γ-glutamyl-L-cysteine + ADP + Pi
2. γ-glutamyl-L-cysteine + glycine + ATP → GSH + ADP + Pi

(Equation 1)

The first reaction is the rate-limiting step marked by the catalysis by glutamate-cysteine ligase (GCL) [46]. GCL is an enzyme composed of two protein subunits: the glutamate-cysteine ligase catalytic (GCLC) subunit (73 kDa), which contains all of the binding sites for catalysis; and the glutamate-cysteine ligase modifier (GCLM) subunit (31 kDa), which does not actively participate in the reaction, but has been found to increase activity of the other subunit [26, 27]. Thiol-containing reductants, such as GSH, and other reagents can cause dissociation of GCLC and GCLM, thereby downregulating GCL in the presence of excess GSH [29]. Additionally, GCLC and GCLM transcription is upregulated by the presence of electrophiles or oxidative stress [30].

The second step of the reaction is catalyzed by GSH synthase (GS) (118,000 kDa) and acts relatively quickly on the intermediate γ-glutamyl-L-cysteine moiety [31]. Overexpression of GS does not affect GSH levels as GCL does--enforcing the idea that the

GCL catalysis is indeed the rate limiting step--and GS is not subject to feedback inhibition by GSH [32].

2.1 Regulation by GCL

GCL availability is considered to be a major factor in GSH synthesis. As previously mentioned, GCL's protein subunit GCLC is responsible for most of the activity of GCL. GCLC expression can be regulated by transcription, which has shown to be induced by treatment with insulin [35]; induced by treatment with hydrocortisone [36]; induced by rapid cell growth during general proliferation and during hepatocellular carcinoma [46]; regulated by chronic inflammatory disorders, pulmonary fibrosis, liver fibrosis [37]; induced by cysteine deprivation [38]; and many other factors. Essentially, GCLC is induced to increase cellular defense against unfavorable states and is found to be hampered in disease states.

GCLM, the lighter subunit of GCL that increases the efficiency of GCL as a whole, is typically up-regulated at the same time as its partner, GCLC, though special scenarios do exist where GCLM up-regulation is favored [46].

2.2 Regulation by Availability of Amino Acids

In addition to GCL availability, GSH synthesis is limited by the availability of the amino acid, cysteine ($C_3H_7NO_2S$). Cysteine is obtained mostly from the diet, breakdown of proteins, and synthesis via methionine in the liver. Cysteine behaves such that it is in a

sulfhydryl form, cysteine, inside the cell and in a disulfide form, cystine ($C_6H_{12}N_2O_4S_2$) outside of the cell due to cysteine's autoxidizing in the extracellular fluid and cystine's reduction upon entering the cell [33, 34]. Hence, it can be said that, assuming an adequate diet, cystine's transport across the membrane and into the cell is an important factor of cysteine availability.

The aforementioned synthesis of cysteine via methionine ($C_5H_{11}NO_2S$) in the liver is due to methionine cycling and the transulfuration pathway, and is only significant in hepatic cells. Since the experimental cellular model that serves as the basis for this paper was hepatoma cells, the contribution of methionine to cysteine availability is included.

2.3 Glutathione as an Indicator of Cellular Stress

As previously discussed, GSH has been implicated as aiding the body in a large variety of applications. Cellular concentration of GSH may rise and fall as the cell responds to stress, which may come in the form of ROS, drugs, toxins, and pollutants. For example, peroxide (H_2O_2) reacts with glutathione peroxidase with two molecules of GSH acting as an electron donor in the reduction reaction [14], producing the oxidized state of GSH denoted as GSSG. The reaction is given:

$$2GSH + ROOH \rightarrow GSSG + ROH + H_2O \qquad \text{(Equation 2)}$$

This kind of reaction that converts a supply of GSH into other forms reflects how GSH responds to cellular stress. Therefore, when GSH concentrations decrease, it is indicative of the cell undergoing stress.

CHAPTER 3

In Vivo Experimental Measurements

Experimental data was collected using Carbon-13 nuclear magnetic resonance (^{13}C NMR) so as to study glutathione metabolism in cultured cells using a noninvasive *in vivo* detection. ^{13}C NMR enables direct monitoring of metabolic pathways and pharmacodynamic data in intact tissues.

3.1 Experimental Method

The cell culture was obtained by using JM1 rat hepatoma cells cultured in Dulbecco's modified Eagles medium (DMEM) supplemented with 10% fetal bovine serum containing streptomycin and penicillin.

Labeled cystine and unlabeled methionine were added to cysteine- and methionine-deficient DMEM to create labeled growth media.

In order to conjugate glutathione, 2mM monobromobimane (mBBr) in dimethyl sulfoxide (DMSO) was added to labeled growth media.

Cells were encapsulated in solid calcium alginate beads and transferred to culture media in an NMR-compatible bioreactor. For the first 17 hours, the cells were allowed to uptake the labeled cystine. At 17 hours, the cells were exposed to mBBr media for 10 minutes before returning to mBBr-free ^{13}C-DMEM. ^{13}C NMR spectral acquisitions were then obtained at 1.2 minute intervals for 6 hours.

3.2 Experimental Results

The resulting spectra described GSH levels and GSH - mBBr conjugates (GSBi) versus time. Since the behavior of glutathione metabolic dynamics were determined experimentally, any discrepancies between model fits and experimental data required adjustments to be made in the model--including reconsidering its assumptions, equations, and relationships--to produce a good fit.

The experiment was carried out twice and the data--GSH levels and GSBi levels measured at intervals of 1.2 minutes--were generated. The normalized results for data sets 1 and 2 are presented in Figures 3.1 and 3.2, respectively.

In the dataset presented in Figure 3.1, mBBr dosage occurs at 17 hours and GSBi levels and GSH levels reach their maximum and minimum values, respectively, at approximately 17.5 hours. Then, until the end of the data at approximately t=21 hours (or 4 hours after aftermBBr dose), GSH levels are gradually restored and GSBi is removed from the system.

The dataset presented in Figure 3.2 displays similar behavior and time points as data set 1. However, the data points exhibit a visually wider spread.

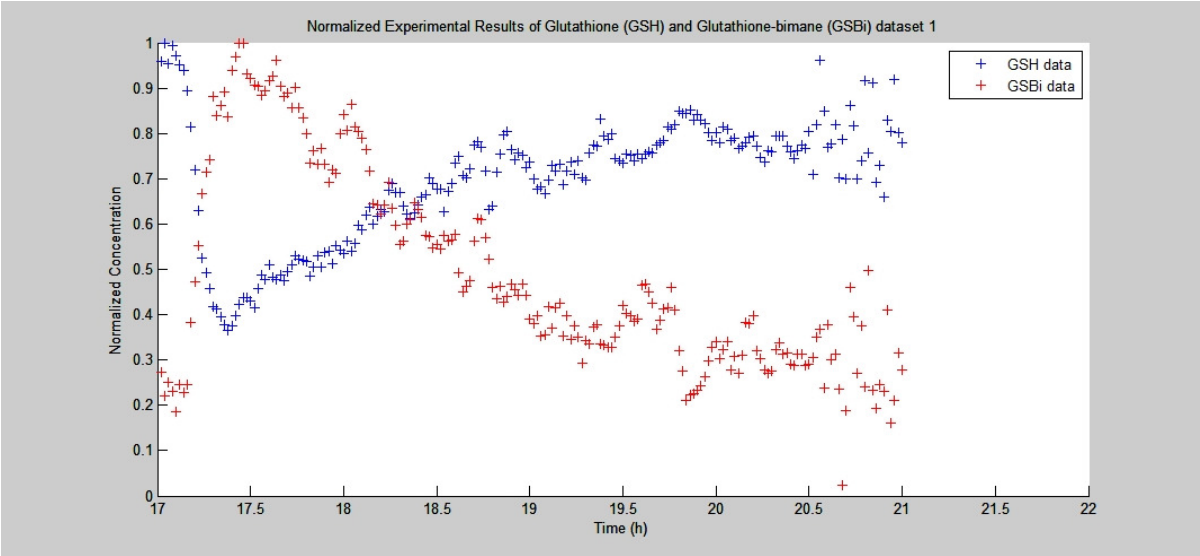

Figure 3.1. Experimental Results from Data Set 1

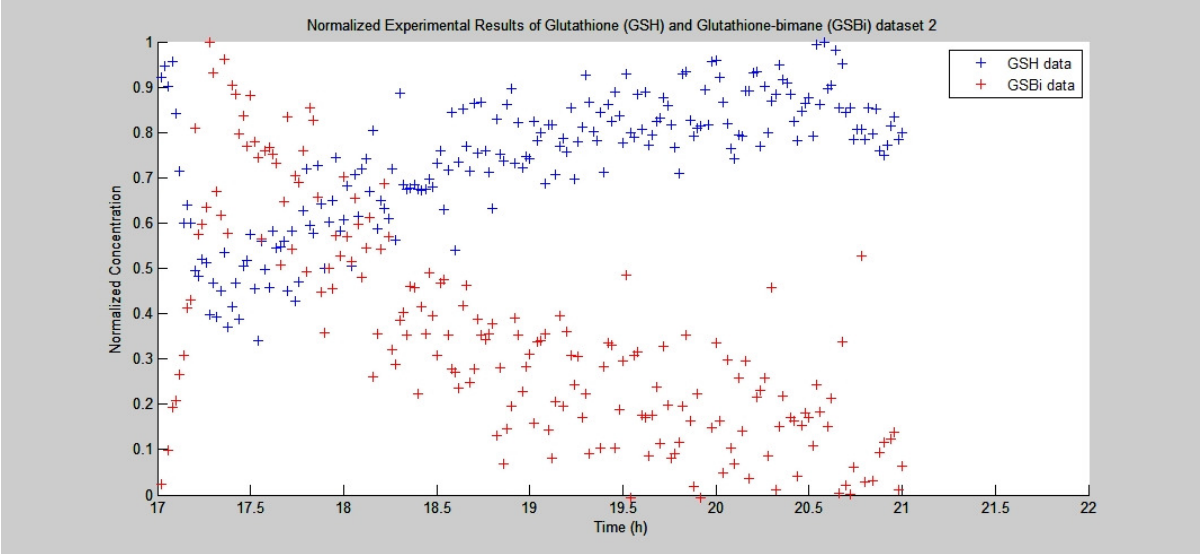

Figure 3.2. Experimental Results from Data Set 2

CHAPTER 4

Mathematical Modeling

The work of Reed et al. [39] forms the basis of much of the mathematical modeling of glutathione synthesis in hepatic cells which was reproduced in SimBiology, a biochemical pathway simulator by MathWorks. Their work provides a framework with which we will then examine how mBBr depletes cellular GSH concentrations, GSH feedback inhibition is released, and normal cellular concentrations are restored.

The model is composed of two compartments, the blood compartment and the cellular compartment. Experimentally, the blood compartment is replaced by cell culture media as discussed in Section 3.1, because media as an environment is easier to manipulate and control. As media acts as a surrogate for blood and to parallel the terminology of Reed et al., we will continue to refer to it as the blood compartment.Figure 4.1 shows a diagram of the model and the biochemical pathways represented in SimBiology. Reaction parameters are given in the appendix of this paper and discussed in the following sections.

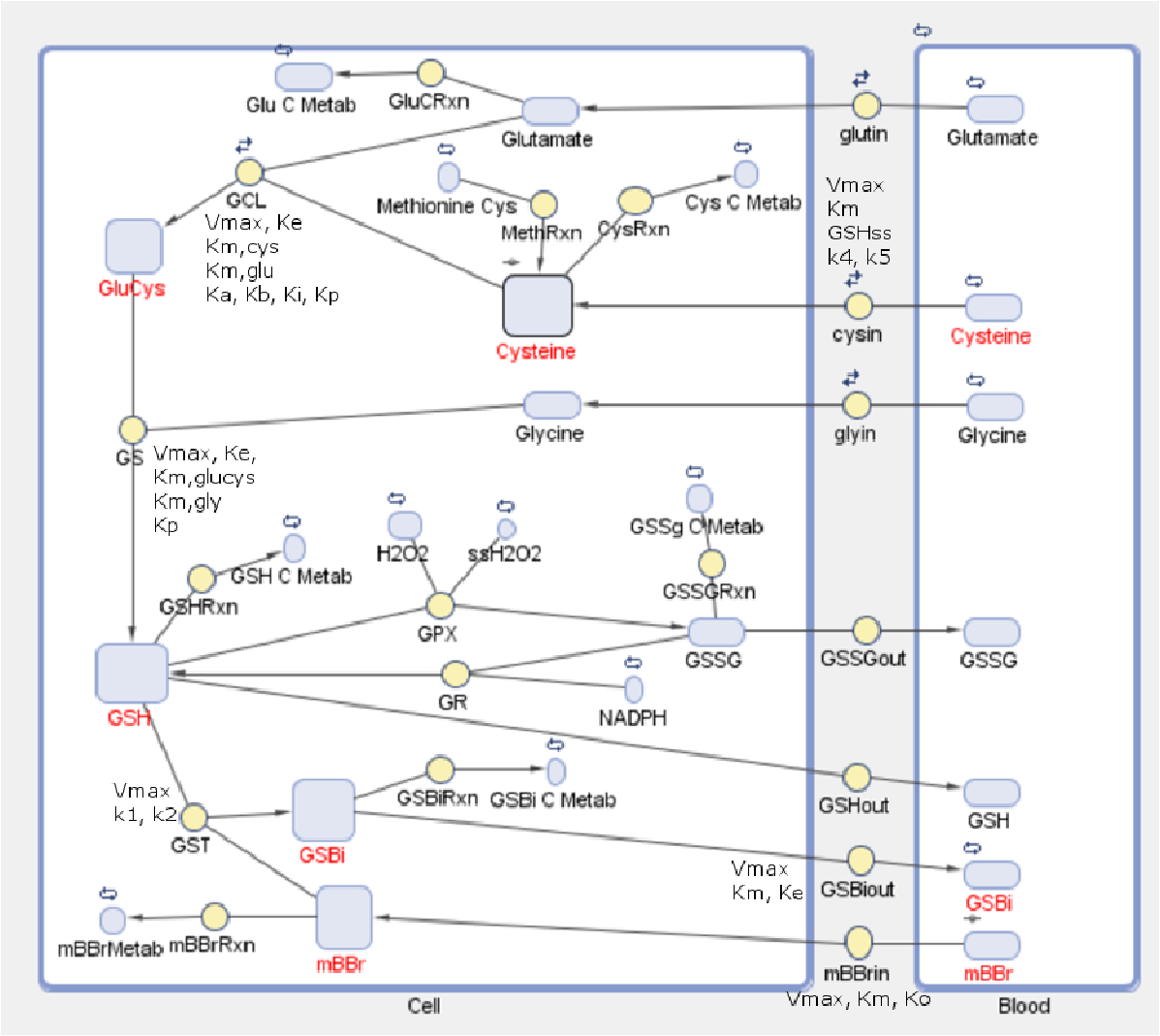

Figure 4.1. Diagram of SimBiology Model. We consider the blood compartment on the right and the cell compartment on the left. Blue rounded rectangles denote species. Blue circles denote sources or sinks. Yellow circles denote reactions for which there are programmed reaction rate equations. Important species discussed in this paper are denoted with red text and their reactions also list corresponding parameters. Abbreviations for various species are given throughout the text and in the List of Abbreviations. For those not listed, shorthand is given as follows: Metab, Metabolism; Rxn, Reaction; AA, Amino Acid; Meth, Methionine; Cys, Cysteine; C, Cellular; Cys, Cysteine; Gly, Glycine; Glut, Glutamate.

4.1 Equations

We will begin examining the model starting with the amino acids in the blood compartment. Many of these equations will be discussed in detail in section 4.2 and, in the case of equations 5 and 6, section 4.4.

Cysteine, glycine, and glutamate concentrations in the blood were set as constants, as the volume of media was comparatively larger than that of the encapsulated cells. The amino acids, glycine and glutamate (abbreviated to gly and glu in the equations, respectively), transport across the cell membrane into the cytosol at the following reaction rates:

$$V_{gly,in} = \frac{V_m[gly_B]}{(K_m + [gly_B]) - (K_o[gly_C])} \qquad \text{(Equation 3)}$$

$$V_{glu,in} = \frac{V_m[glu_B]}{(K_m + [glu_B]) - (K_o[glu_C])} \qquad \text{(Equation 4)}$$

where the subscripts B and C refer to the corresponding substrate's concentration in the blood and cytosol, respectively.

The reaction rate for cysteine transport into the cell uses similar mechanics, but has an added term to consider GSH concentration (which will be discussed in Section 4.4):

$$V_{cys,in} = \frac{V_{\max}[cys_B]}{K_m + [cys_B]} \left(\frac{(k_4 + k_5)[GSH_{ss}]^2}{[GSH_{ss}]^2 k_4 + [GSH_C]^2 k_5}\right) \qquad \text{(Equation 5)}$$

Glutamate and cysteine are catalyzed by GCL to react and form gamma-glutamyl-cysteine (GluCys), and the process is governed by the reaction rate:

$$V_{GCL} = \frac{V_{\max}([glu_C][cys_C] - \frac{[GluCys]}{K_e})}{K_{m,cys}K_{m,glu} + K_{m,cys}[glu_C] + K_{m,glu}[cys_C](1 + \frac{[GSH_C]}{K_i} + \frac{[glu_C]}{K_{m,glu}}) + \frac{[GluCys]}{K_p} + \frac{[GSH_C]}{K_i}) * \frac{K_a + [ssH_2O_2]}{K_a + [H_2O_2]} * \frac{K_b + [mBBr_C]}{K_b}}$$

(Equation 6)

which is then quickly catalyzed by GS (aided by glycine) to form GSH via the reaction rate:

$$V_{GS} = \frac{V_{\max}([gly_C][GluCys] - \frac{[GSH_C]}{K_e}}{K_{m,GluCys}K_{m,gly} + K_{m,gly}[GluCys] + K_{m,GluCys}[gly_c](1 + \frac{[GluCys]}{K_{m,GluCys}}) + \frac{[GSH_C]}{K_p}}$$

(Equation 7)

Through one pathway, some of GSH is exported from the cell to the blood via the following kinetics:

$$V_{GSH \to blood} = \frac{V_{\max,H}[GSH_C]}{K_{m,H} + [GSH_C]} + \frac{V_{\max,L}[GSH_C]^3}{K_{m,L}{}^3 + [GSH_C]^3}$$ (Equation 8)

GSSG, an indicator for oxidative stress, follows similar kinetics with the additional consideration of reactive oxygen species concentration

$$V_{GSSG \to blood} = \frac{V_{\max,H}[GSSG_C]}{(K_{m,H} + [GSSG_C])\frac{K_H + [H_2O_2]}{K_H + [ssH_2O_2]}} + \frac{V_{\max,L}[GSSG_C]}{(K_{m,L} + [GSSG_C])\frac{K_L + [H_2O_2]}{K_L + [ssH_2O_2]}}$$

(Equation 9)

Turning once again to the blood compartment, as per the experimental conditions, monobromobimane (mBBr) is dosed to the system, which crosses the cellular membrane by the reaction rate:

$$V_{mBBr\rightarrow cell} = \frac{V_{\max}[mBBr_B]}{K_m + [mBBr_B] - K_o[mBBr_C - mBBr_B]} \qquad \text{(Equation 10)}$$

mBBr is scavenged by GSH by the process of mBBr alkylating GSH's thiol group. This process forms a GSH-mBBr conjugate, GSBi, according to the equation:

$$V_{GST} = \frac{V_{\max}[GSH_C][mBBr_C]}{k_1 k_2 + k_2[GSH_C] + k_1[mBBr_C] + [GSH_C][mBBr_C]} \qquad \text{(Equation 11)}$$

To detoxify the cell, while some GSBi is naturally metabolized within the cell at a slow rate, the bulk removal of GSBi occurs through the cellular membrane and into the blood compartment by the reaction rate:

$$V_{GSBi\rightarrow blood} = \frac{V_{\max}[GSBi_C]}{K_m + [GSBi_C] - K_e[GSBi_B]} \qquad \text{(Equation 12)}$$

4.2 Analysis of Kinetics

Many of the reaction rates given follow a standard model in the form of Michaelis-Menten kinetics. Michaelis-Menten kinetics considering only one substrate are of the form

$$V = \frac{V_{\max}[S]}{K_m + [S]} \qquad \text{(Equation 13)}$$

However, this model considers the transport of amino acids to be reversible. While abundant research has characterized the transport of amino acids into the cell, little is known

about the kinetics of amino acids leaking out of cells, so we assume the kinetics of amino acid leakage to be linear [39]. Therefore, reversible single substrate equations with $[S_B]$denoting the substrate concentration in the blood and $[S_C]$ denoting the substrate concentration in the cytosol gives

$$V = \frac{V_{\max}[S_B]}{(K_m + [S_B]) - K_{out}[S_C]} \qquad \text{(Equation 14)}$$

Random order Michaelis-Menten kinetics considering two substrates are of the form

$$V = \frac{V_{\max}[S_1][S_2]}{(K_{m,1} + [S_1])(K_{m,2} + [S_2]} \qquad \text{(Equation 15)}$$

The kinetics for V_{GCL} (Equation 6) are reversible and GSH is a competitive inhibitor of GCL against glutamate, thereby slowing the kinetics of GCL when GSH is abundant [39]. The form for V_{GCL} was given by Mendoza-Cozatl et al. [41] and the constants are given by Reed et al. [39]. $K_{m,\ cys}$=100μM and $K_{m,\ glut}$=1900μM are the kinetic constants for cysteine and glutamate, respectively. K_e=5597μM is the equilibrium constant for the breakdown of the enzyme-GluCys complex. K_i=8200μM is the inhibition by GSH constant. K_p=300μM is the dissociation constant of glutamyl-cysteine. And the maximum rate of the equation is V_{max}=3600μM/h. The last factor represents activation of GCL by oxidative stress, where K_a=0.01μM is the activation constant, ssH_2O_2=0.01μM is the steady state concentration of H_2O_2, and H_2O_2=0.01μM is the concentration for an experiment. Reed et al. used this equation to model oxidative stress. Because in this model, cellular stress is experimentally applied mBBr and the effect created by mBBris much greater than the normal low-level oxidative stress present in cells, the ratio of H_2O_2 and ssH_2O_2 is set to 1 to ignore the term.

The kinetics for V_{GS} (Equation 7) is a reversible bi-reactant Michaelis-Menten form given by Mendoza-Cozatl et al. [41]. K_m^{GluCys}=22µM and K_m^{gly}=300µM are the kinetic constants for GluCys and glycine, respectively. K_p=30µM is the dissociation constant for GSH. K_e=5600µM is the equilibrium constant. And V_{max}=5400µM/h.

The equation for GSH export from the cytosol to the blood (Equation 8) has been derived from studies of the kinetics in rat livers [42]. It involves high and low affinity, high capacity transporters that operate via different kinetics. The high affinity transporter uses Michaelis-Menten kinetics with V_{max}=150µM/h and K_m=150µM. The low affinity transporter uses sigmoidal kinetics with V_{max}=1100µM/h, K_m=3000µM, and Hill coefficient=3. Therefore, it can be seen in Equation 8 that it is the sum of the two kinetic models.

The equation for GSSG export from the cytosol to the blood (Equation 9) follows a similar construction as above. The high affinity transporter for GSSG has V_{max}=40µM/h and K_m=1250µM. The low affinity transporter for GSSG has V_{max}=4025µM/h, K_m=7100µM. Oxidative stress would normally be represented in this equation, modulating the export of GSSG in the terms seen in the denominator. In this paper, cellular kinetics are manipulated via mBBr, which is given an independent rate equation. Hence, oxidative stress will be ignored in this scenario, setting H_2O_2 concentration and steady state H_2O_2 concentration equal to each other, thereby reducing the relevant terms to 1.

4.3 Generation and Metabolism

Additionally, there is generation (external input) of substrates and metabolism (external output) of substrates where "external" simply refers to sources and sinks that are not accounted for in the model. Typically, nutrition is primarily responsible for the input of amino acids. Metabolism is the general term used here to describe loss of a substrate to natural breakdown. Various sources and sinks are implemented throughout the cell compartment of the model and can be seen in Figure 4.1.

For the amino acids in the blood compartment, mimicking the experimental conditions in which the cells were submerged in a relatively large amount of media, we shall assume that amino acid concentrations are constant.

4.4 Feedback and Inhibition

There are two feedback mechanics that are incorporated in the equations. The first is a negative feedback loop from GSH to cysteine uptake into the cell implemented because, in preliminary models, it was found that modeled cysteine uptake was inadequate for GSH recovery (this will be demonstrated in Section 5.3). This feedback loop is the reason that the transport of cysteine into the cell has a reaction rate different than that of glutamate and glycine. The reaction rate was previously given in Equation 5 as

$$V_{cys,in} = \frac{V_{\max}[cys_B]}{K_m + [cys_B]} \left(\frac{(k_4 + k_5)[GSH_{ss}]^2}{[GSH_{ss}]^2 k_4 + [GSH_C]^2 k_5}\right) \qquad \text{(Equation 5)}$$

The first term mimics normal Michaelis-Menten kinetics. The second term is added to account for the feedback loop; the $[GSH_C]$ term in the denominator ensures that when

cellular GSH concentration drops, the denominator shrinks, and $V_{cys,in}$ increases. The GSH_{ss} term represents a reference value for GSH. When GSH_C equals GSH_{ss}, the second term reduces to 1 and the equation is then solely dependent on the first term, therefore GSH_{ss} has a larger effect on cysteine uptake when GSH_C is depleted. The other parameters, k_4 and k_5, are constants that control and modulate the effect of this term. The values for the first term were obtained from Reed et al., whereV_{max}=14950μM/h and K_m=2100μM [39]. In preliminary modeling, the values for the second term were estimated ask_4=0.5μM, k_5=2μM, and GSH_{ss} equals4700.

The second feedback loop occurs when GSH is abundant, it inhibits the creation of the GluCys by inhibiting GCL. The reaction rate for the formation of GluCys was given previously as Equation 6

$$V_{GCL} = \frac{V_{\max}([glu_C][cys_C] - \frac{[GluCys]}{K_e})}{K_{m,cys}K_{m,glu} + K_{m,cys}[glu_C] + K_{m,glu}[cys_C](1 + \frac{[GSH_C]}{K_i} + \frac{[glu_C]}{K_{m,glu}}) + \frac{[GluCys]}{K_p} + \frac{[GSH_C]}{K_i})} * \frac{K_a + [ssH_2O_2]}{K_a + [H_2O_2]} * \frac{K_b + [mBBr_C]}{K_b}$$

(Equation 6)

Again, the cellular GSH term appears in the denominator and consequently, a large GSH concentration results in V_{GCL} decreasing (inhibition), and a low concentration of GSH releases that inhibition.

4.5 Literature Review

The references were re-examined in greater detail and it was noticed that there is a discrepancy in the paper published by Reed et al. in *Theoretical Biology and Medical Modelling*and the Supplementary Material they submitted alongside the article. In the main article, the equation for converting GluCys to GSH is given as

$$V_{GS} = \left(\frac{V_{\max}\left(AB - \frac{P}{K_e}\right)}{K_a K_b + K_b A + K_a B\left(1 + \frac{A}{K_a}\right) + \frac{P}{K_p}}\right) \qquad \text{(Equation 16)}$$

where the following substitutions have been made: A=[GluCys], K_a=$K_{m,glucys}$, B=[glycine], K_b=$K_{m,glycine}$, P=[GSH]. There is an unpaired parenthesis following the last term in the denominator. Meanwhile, in the supplemental material by Reed et al., using the same substitutions, the equation appears as

$$V_{GS} = \frac{V_{\max}\left(AB - \frac{P}{K_e}\right)}{K_a K_b + K_b A + K_a B\left(1 + \frac{A}{K_a}\right) + \frac{P}{K_p}} \qquad \text{(Equation 17)}$$

which does not have the unpaired parenthesis. Furthermore, for the equation, Reed et al. cites a paper by Mendoza-Cozatl et al. [41] that gives the equation as

$$V = \frac{\frac{V}{K_a K_b}\left(AB - \frac{P}{K_{eq}}\right)}{1 + \frac{A}{K_a} + \frac{B}{K_b}\left(1 + \frac{A}{K_a}\right) + \frac{P}{K_p}} \qquad \text{(Equation 18)}$$

using the same substitutions. When K_aK_b is multiplied through the denominator, the resulting equation is

$$V = \frac{V(AB - \frac{P}{K_{eq}})}{K_a K_b + K_b A + K_a B(1 + \frac{A}{K_a}) + K_a K_b \frac{P}{K_p}} \qquad \text{(Equation 19)}$$

which differs from the equation given by Reed et al. due to the K_aK_b term multiplied by the last term in the denominator.

Incorporating the $K_aK_b$term in the model actually results in a poorer fit. Instead of the initial fast rise of GSH and then leveling off of the curve seen in Figure 5.1, incorporating K_aK_b into the equations results in a flatter, straighter curve.Our group reached out to Reed et al. for clarification but did not receive a response on the matter. Because the experimental data matches the modeling results when using the equation from Reed et al., the $K_aK_b$term was ultimately omitted and Equation 17 was implemented.

4.6 Comparison of Model to Experimental Data

Figure 4.2 and 4.3 compare the initial mathematical model plotted on the same graphs as the first two sets of experimental data. In Figure 4.4, we consider the normalized average of the two datasets plotted with the model.

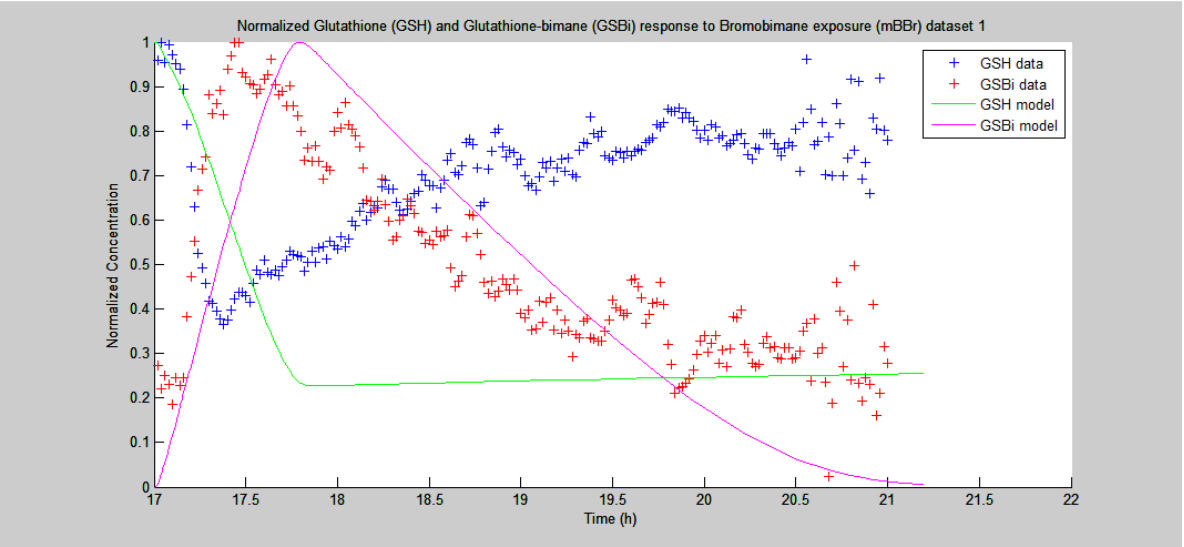

Figure 4.2. Initial Modeled Concentrations Plotted With Data Set 1

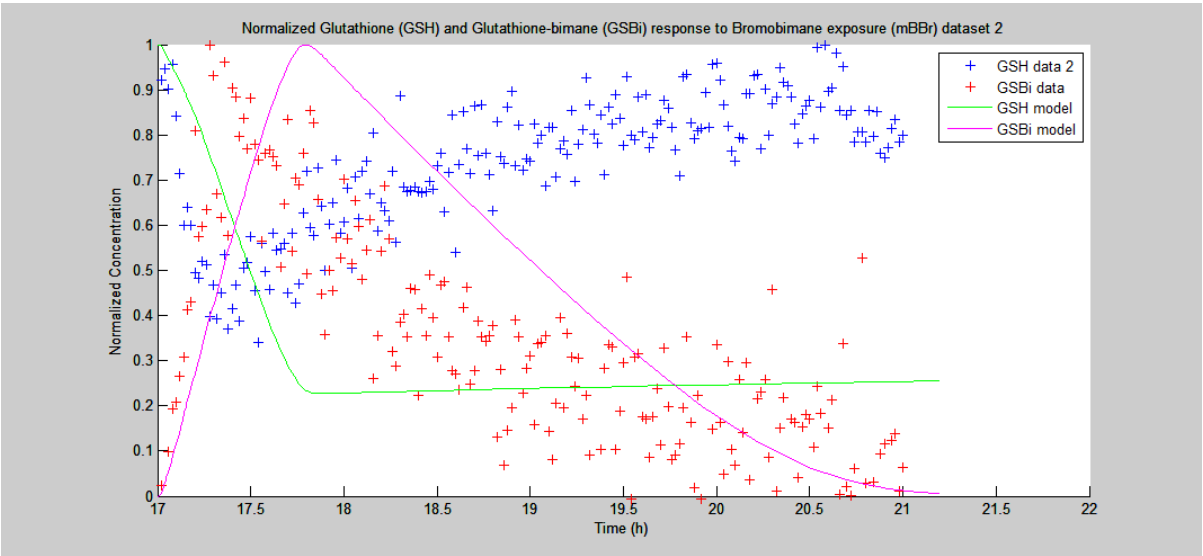

Figure 4.3. Initial Modeled Concentrations Plotted With Data Set 2

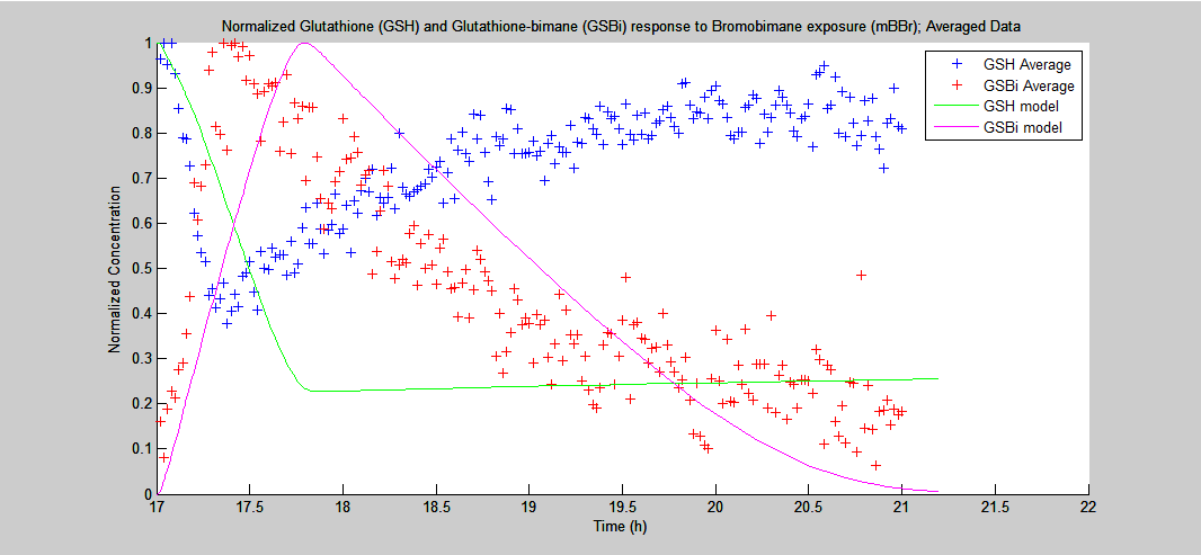

Figure 4.4. Initial Modeled Concentrations Plotted With Average of Data Sets

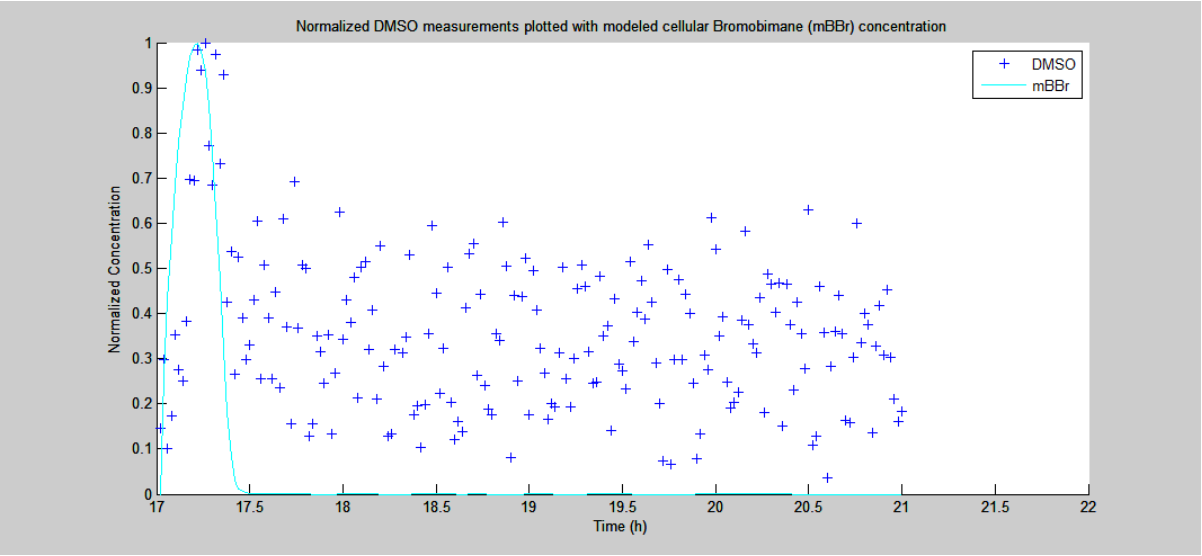

Figure 4.5.Normalized DMSO Measurements Plotted with Modeled mBBr Uptake

Figure 4.5 shows normalized DMSO uptake into the cell as measured by ^{13}C NMR and compares it to the modeled mBBr uptake. As stated in Section 3.1, DMSO was the

vehicle for mBBr in the experiment. There is noise and residual amounts of DMSO for the duration of the experiment, but there is a peak at approximately 17.25 hours indicating introduction into the cell. To achieve this in the model, V_{max}=25,000μM/h in Equation 10 regarding mBBr entry into the cell.

Using the equations and constants described previously in sections 4.1 through 4.4 (and summarized in Appendix A), the resulting plot of concentration for modeled cellular GSH does not behave as expected. Modeled GSH concentration reaches its nadir at approximately 17.8 hours, whereas the experimental GSH did so at 17.38 hours. Afterwards, the modeled GSH recovers to only 25% of the original amount at t=21 hours, whereas the experimental GSH recovered to approximately 80% of original at t=21 hours.

The plot of modeled GSBi behavior peaks at 17.8 hours, while experimental GSBi values peak at 17.4 hours. Then, the modeled GSBi concentration decreases to 1% maximum concentration at the t=21 hours, while experimental GSBi concentration decreases to approximately 20% maximum at t=21 hours.

CHAPTER 5

Fitting the Model to the Data

In this chapter, various parameters in the model will be adjusted to attain a better fit. Then, the presence of feedback mechanisms will be demonstrated by removing relevant terms from the model.

5.1 Fitted Model

Issues seen in the model presented in Figure 4.4 are (a) modeled GSH and GSBi concentrations change too slowly after mBBr exposure (b) modeled GSH does not recover as fast or as much as the experimental GSH (c) modeled GSBi depletes to near zero, unlike experimental GSBi which levels out at an average of approximately 20%.

The parameters affecting modeled GSH and GSBi concentrations were adjusted from the numbers obtained from the references to achieve a better fit of the data.

The primary factors affecting cellular GSH recovery to expected levels are GSH's reaction with mBBr and cysteine levels in both the blood and cytosol which, in turn, affect the availability of GluCys and its catalysis by GSH-synthase to form GSH.

Starting from the transport of cysteine through the cell membrane (Equation 5), the following changes were made to increase the transport: V_{max} changed from 14950µM/h to 16500µM/h, k_4 changed from 0.5µM to 2.5µM, k_5 changed from 2µM to 50µM, and GSH_{ss} changed from 4700µM to 5200µM. Increasing V_{max} increases the maximum rate, increasing GSH_{ss} increases the level at which GSH is regulated, and increasing the k values increases

the relative importance of each accompanying term. Cysteine is one of the first steps in GSH synthesis, so these changes should help with the overall recovery of GSH levels.

Cysteine is consequently combined with glutamate to form GluCys via Equation 6. V_{max} was changed from 3600µM/h to 4500µM/h, thereby increasing the rate of this reaction so that GluCys is available to synthesize GSH, increasing the recovery of GSH concentration.

In the reaction between GSH and mBBr (Equation 11), V_{max} was changed from 8950µM/h to 16900µM/h. This increases the rate at which mBBr depletes GSH concentration, which in turn increases the initial rate of formation of GSBi. As the experimental results exhibited a faster reaction time between GSH and mBBr, this should align the model with the experiment.

Additionally, to address GSBi concentration (Equation 12), K_m was changed from 500µM to 3900µM, and V_{max} was changed from 2000µM/h to 3500µM/h. This balance decreases the efficiency with which GSBi is moved out of the cellular compartment, slowing the rate of GSBi depletion to align with the experiment.

5.2 Model Results

Figure 5.1 shows the results of these changes and Figure 5.2 is a plot of the residuals.

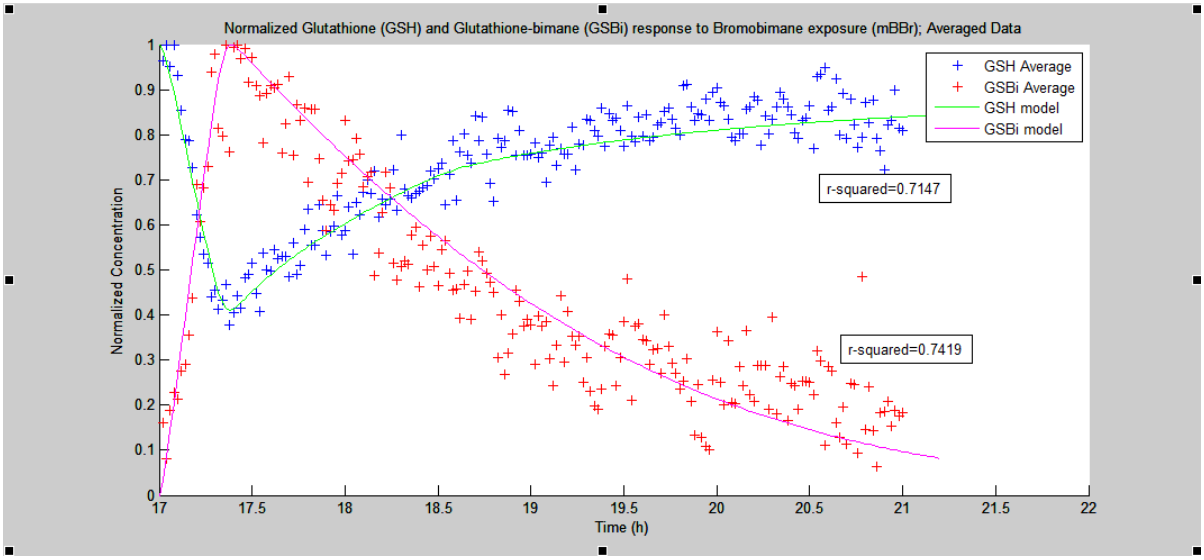

Figure 5.1. Fitted Model Plotted with Averaged Data Sets.

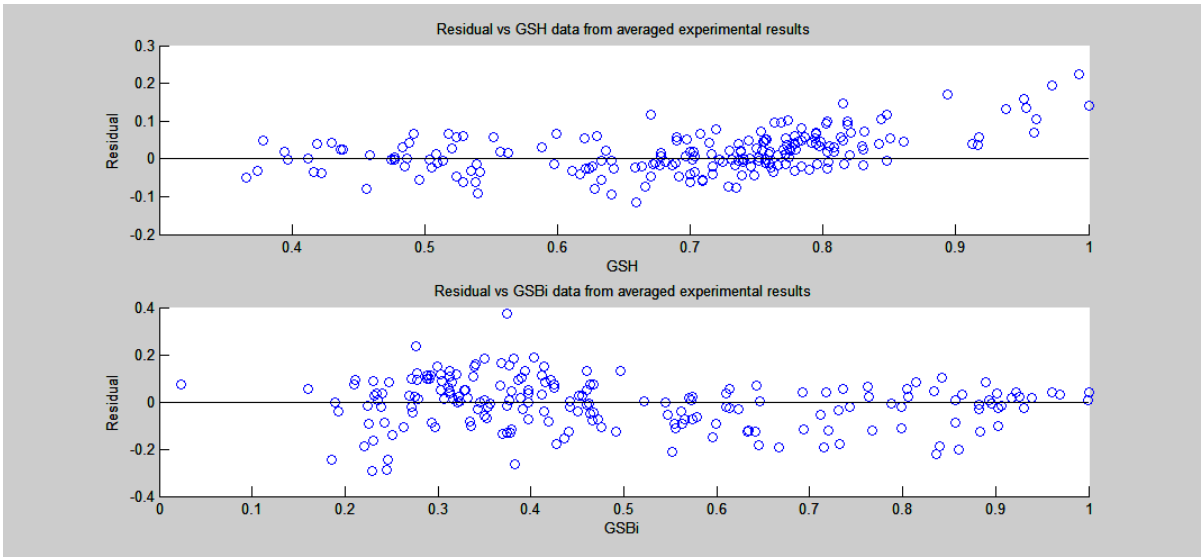

Figure 5.2. Residuals of Fitted Model vs Substrate.

Both modeled GSH and modeled GSBi mimic experimental conditions well with correlation coefficient (r^2) values of 0.7147 and 0.7419, respectively. They are both significant improvements over Figure 4.4 because the initial depletion of GSH and increase

of GSBi occur at the same rate and display good recovery of GSH (84% recovery of max GSH) and removal of GSBi(10% left of peak GSBi) at t=21 hours.

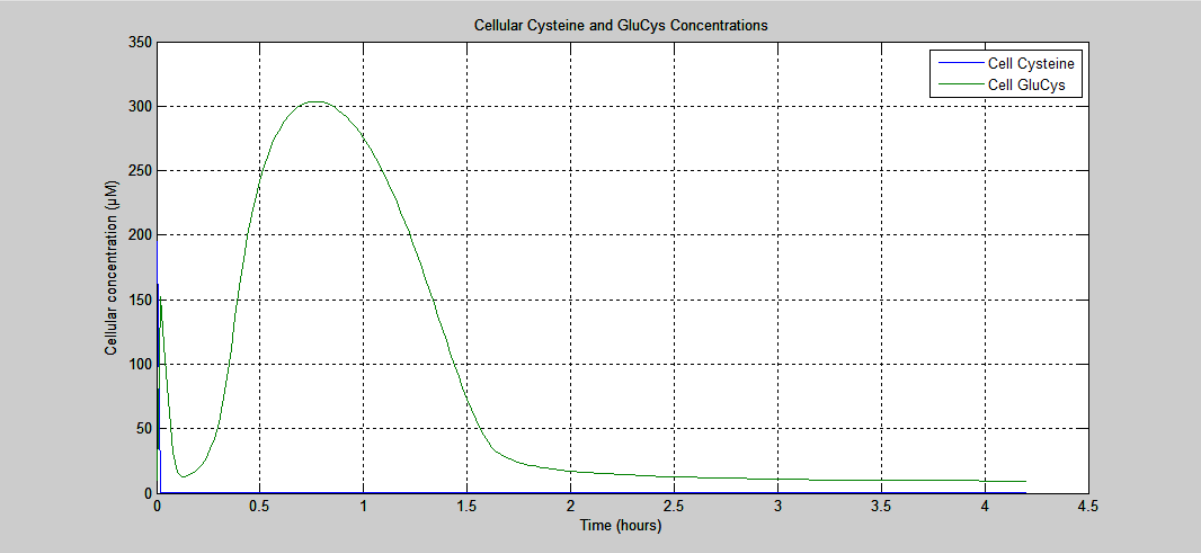

Figure 5.3. GluCys and Cysteine Concentrations in the Cytosol. Here, t=0 corresponds to the experimental time of t=17 hours when mBBr dosage occurred.

Figure 5.3 shows how cellular concentrations of GluCys (green) and cysteine (blue) behave after mBBr dosing. GluCys concentration drops as GSH is depleted, indicating that all available GluCys is rapidly converted to GSH in response to mBBr exposure. As GSH concentration continues to drop to its nadir at approximately 0.38 hours after dosing, GluCys concentration rises. This demonstrates the release of GCL inhibition via GSH that was discussed in Section 4.4. As GSH concentration recovers, it uses the available GluCys and then GluCys formation is once again inhibited when GSH is high again, driving GluCys concentration back toward its initial concentration of 9.8µM.

The immediate drop of cellular cysteine to near-zero levels demonstrates that enhancing cysteine uptake as described in Section 5.1 was necessary. Figure 5.4 is a

zoomed-in view of cysteine concentrations. It is seen that after dropping to near-zero, cellular cysteine concentration recovers sharply, though briefly. This demonstrates how lower GSH concentrations increases cysteine uptake into the cell as discussed in Section 4.4. As GSH levels recover, cysteine is consumed, depleting the concentration once again.

The model shows that cysteine concentrations do not rise again during the course of the experiment despite GCL inhibition returning when GSH levels rise. This could be indicative of both the criticality of cysteine for GSH synthesis and the relative weakness of the GCL inhibition (this will be shown in Section 5.3, where there is a relatively minor difference with and without GCL inhibition).

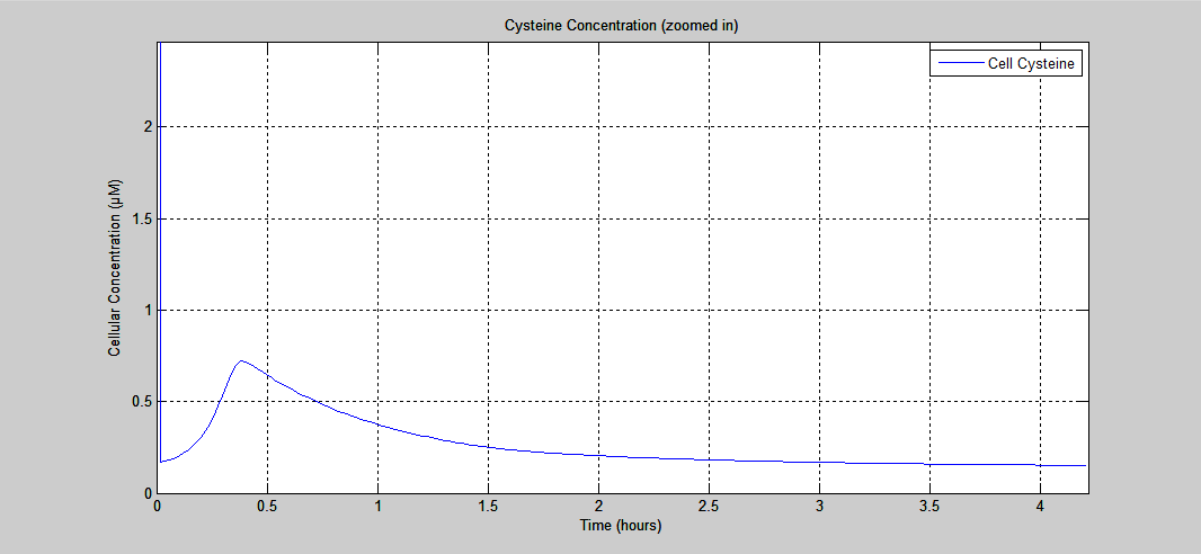

Figure 5.4. Cysteine Concentrations in the Cytosol. Here, t=0 corresponds to the experimental time of t=17 hours when mBBr dosage occurred.

5.3Demonstration of Cysteine Feedback

Equation 5,describing cysteine transport into the cell,is

$$V_{cys,in} = \frac{V_{\max}[cys_B]}{K_m + [cys_B]}\left(\frac{(k_4 + k_5)[GSH_{ss}]^2}{[GSH_{ss}]^2 k_4 + [GSH_C]^2 k_5}\right) \qquad \text{(Equation 5)}$$

The second term allows for more cysteine uptake when GSH is low. To demonstrate the effect, we removed the second term, leaving just

$$V_{cys,in} = \frac{V_{\max}[cys_B]}{K_m + [cys_B]} \qquad \text{(Equation 20)}$$

and graphed the result to obtain Figure 5.5.

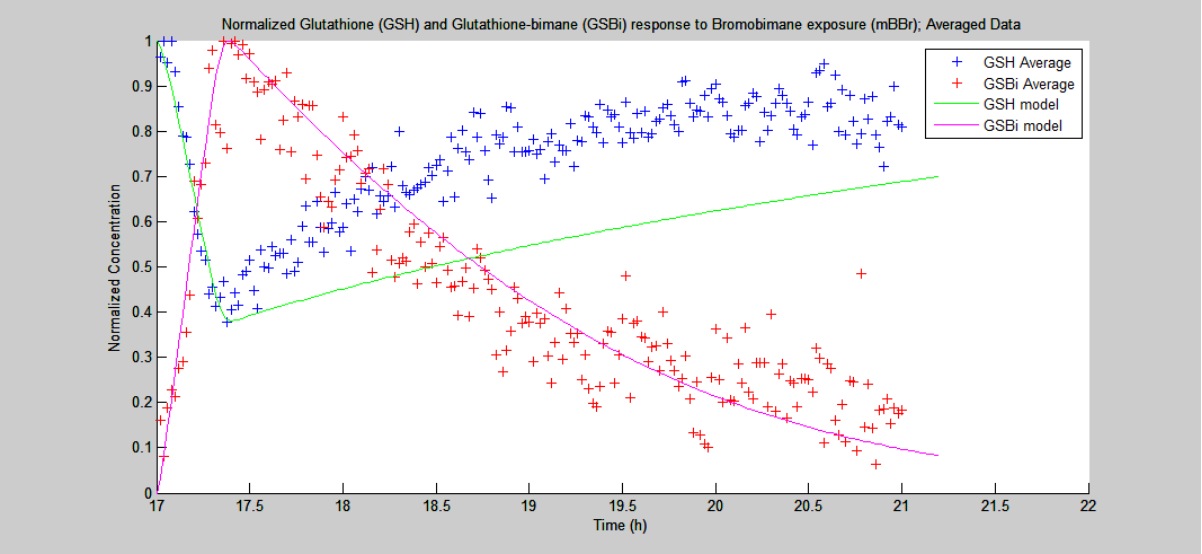

Figure 5.5. Model Without Cysteine Feedback.

It can be seen that recovery of GSH is slow and inadequate because it does not have enough cysteine, which is critical in forming GluCys and subsequently GSH. Furthermore, it should be noted that Figure 5.5 represents the extent to which the model by Reed et al. [39]

might represent our experimental data, as their model does not include the cysteine feedback control.

5.4 Demonstration of GCL Feedback

Equation 6, describing GluCys formation via glutamate and cysteine, is

$$V_{GCL} = \frac{V_{\max}([glu_C][cys_C] - \frac{[GluCys]}{K_e})}{K_{m,cys}K_{m,glu} + K_{m,cys}[glu_C] + K_{m,glu}[cys_C](1 + \frac{[GSH_C]}{K_i} + \frac{[glu_C]}{K_{m,glu}}) + \frac{[GluCys]}{K_p} + \frac{[GSH_C]}{K_i})} * \frac{K_a + [ssH_2O_2]}{K_a + [H_2O_2]} * \frac{K_b + [mBBr_C]}{K_b}$$

(Equation 6)

GSH in the denominator limits the amount of GluCys that is synthesized when GSH is high and allows for more GluCys when GSH is low. To demonstrate this effect, we removedthe GSH terms from the equation, leaving

$$V_{GCL} = \frac{V_{\max}([glu_C][cys_C] - \frac{[GluCys]}{K_e})}{K_{m,cys}K_{m,glu} + K_{m,cys}[glu_C] + K_{m,glu}[cys_C](1 + \frac{[glu_C]}{K_{m,glu}}) + \frac{[GluCys]}{K_p})} * \frac{K_a + [ssH_2O_2]}{K_a + [H_2O_2]} * \frac{K_b + [mBBr_C]}{K_b}$$

(Equation 21)

Using Equation 21, which has no GCL feedback mechanism, we graphedGluCys concentration to produce Figure 5.6.

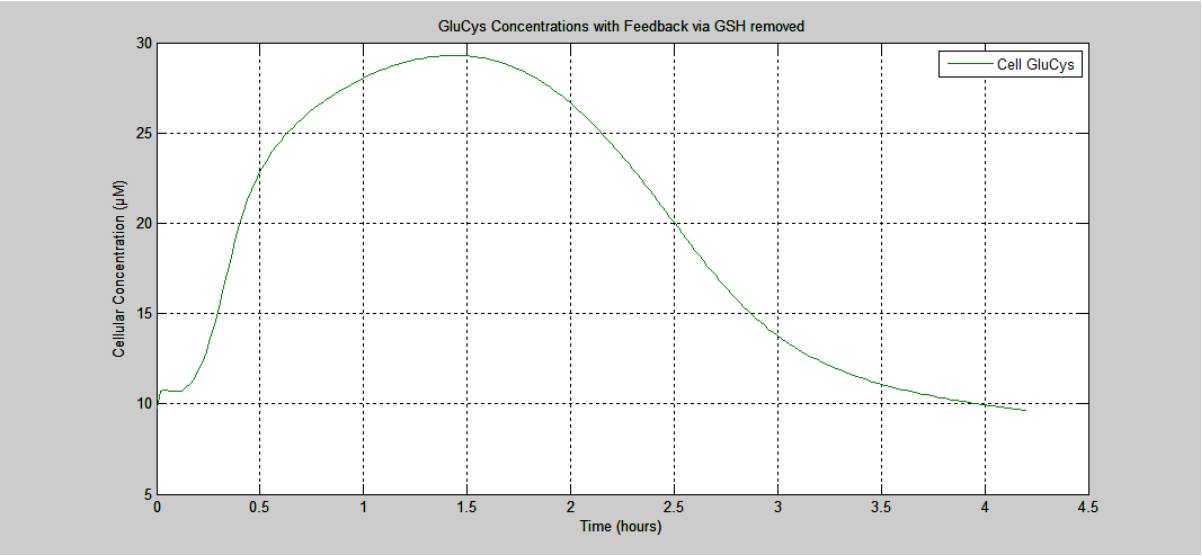

Figure 5.6. GluCys Concentration with GCL Feedback via GSH Removed. Here, t=0 corresponds to the experimental time of t=17 hours when mBBr dosage occurred.

In Figure 5.6, when there is no GCL feedback, we see that GluCys concentration exhibits only 10% of the rise shown in Figure 5.3. Also, the relatively elevated GluCys concentrations remain high for longer. In Figure 5.6, GluCys returns to the initial concentration after 4 hours. In Figure 5.3, GluCys returns to the initial concentration after approximately 2 hours. Hence, when GCL feedback is removed, high GSH concentrations do not inhibit GCL and low GSH concentrations did not release inhibition of GCL.

As a result of removing GSH feedback to GCL, Figure 5.7 shows that modeled GSH does not recover as quickly as experimental GSH. However, this effect is much less pronounced than when the cysteine feedback mechanism was removed in Section 5.3.

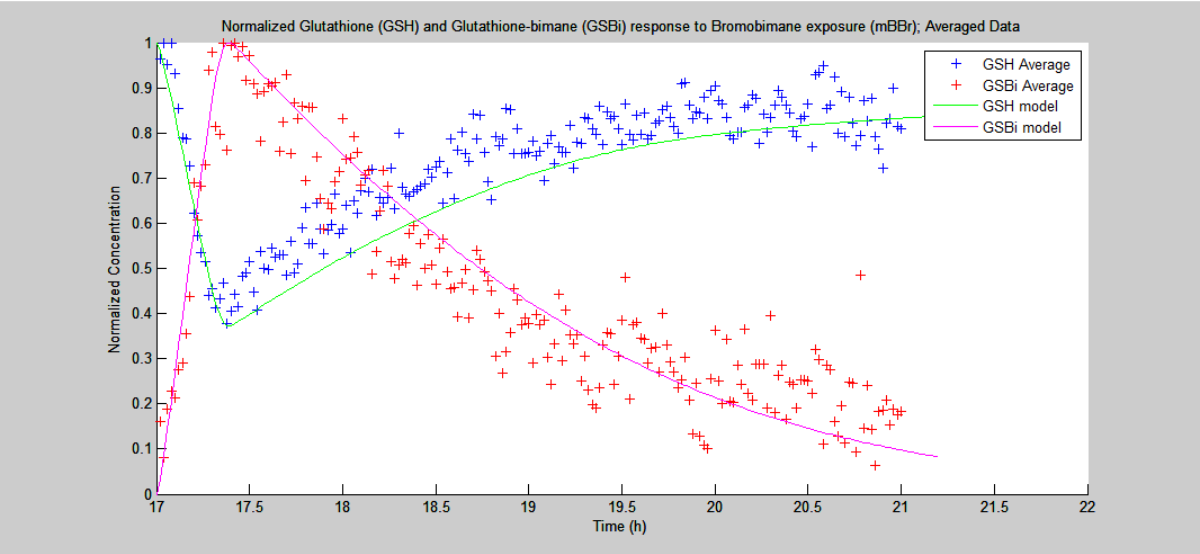

Figure 5.7. GSH and GSBiConcentrations withGCL Feedback Removed.

CHAPTER 6

Review and Future Work

It was shown that the parameters given by Reed et al. [39] did not accurately model GSH and GSBi behavior in JM1 rat hepatoma cells exposed to monobromobimane. In order to fit the model to the experimental data, parameters affecting cysteine transport into the cell and GluCys formation from cysteine and glutamate were changed to increase the rates of the reactions. Additionally, beyond the work of Reed et al., a feedback mechanism whereby low GSH concentrations increase cysteine transport into the cell was implemented. This is a feature which had been suggested by preliminary modeling work done with the experimental data when cysteine concentrations were not adequate for GSH recovery.

There is a second feedback mechanism--one which Reed et al. had indicated--regarding GSH feedback inhibition, which inhibits glutamate-cysteine ligase and the formation of gamma-glutamyl-cysteine when GSH concentrations are high (and, mathematically, up-regulates glutamate-cysteine ligase when GSH concentration is low).

Both feedback mechanisms are then demonstrated by the removal of their respective terms. When either mechanism is excluded, modeled GSH does not replicate experimental data, though the exclusion of cysteine feedback has a much more pronounced effect.

Cysteine up-regulation via GSH feedback is an interesting mechanic that appeared out of necessity for this JM1 rat hepatoma cell model exposed to monobromobimane and introduces a feedback mechanic not present in any previous model found during

literaturereview. Without this mechanism linking GSH to cysteine, the previous models (such as that by Reed et al.) are unable to accurately model our experimental data; Figure 5.5 represents the best possible fit without this feedback. Further research into cysteine transport into the cell under cellular stress could provide greater illumination of the subject, potentially exposing the biological mechanism of action.

Additionally, a wider review of currently available literature should be performed to determine if the given equations are in line with published models and to resolve the differences shown between previously published works.

REFERENCES

1. Morrell CN. "Reactive Oxygen Species - Finding the Right Balance." *Circ Res* (2008): 103(6): 571-572.

2. Alfadda AA; Sallam RM. “Reactive Oxygen Species in Health and Disease.” *J Biomed Biotechnol*(2012): Article 936486.

3. Novo E, Parola M. “Redox mechanisms in hepatic chronic wound healing and fibrogenesis.” *Fibrogenesis& Tissue Repair* (2008):1:5.

4. Berg JM, Tymoczko JL, Stryer L. *Biochemistry. 5th ed*. 2002.

5. Alberts B, Johnson A, Lewis J. *Molecular Biology of the Cell. 4th ed*. 2002

6. Lane N. "Why are Cells Powered by Proton Gradients?" *Nature Education* (2010): 3(9):18

7. Chance B, Sies H, Boveris A. "Hydroperoxide metabolism in mammalian organs" *Physiol Rev* (1979): 59: 527-605.

8. Staniek K, Nohl H, "H_2O_2 detection from intact mitochondria as a measure for one-electron reduction of dioxygen requires a non-invasive assay system." *BiochimBiophysActa*(1999): 1413(2): 70-80.

9. Madamanchi N, Runge M. "Mitochondrial dysfunction in atherosclerosis." *Circ Res* (2007): 100(4): 460-73.

10. Szabo C, Ohshima H. "DNA damage induced by peroxynitrite: subsequent biological effects." *Nitric Oxide* (1997): 1(5): 373-385.

11. Szabo C. "DNA strand breakage and activation of poly-ADP ribosyltransferase: a cytotoxic pathway triggered by peroxynitrite." *ProcNatlAcad Sci USA* (1996): 93:5 1753-1758.

12. Li X, Fang P, Mai J, et al. "Targeting mitochondrial reactive oxygen species as novel therapy for inflammatory diseases and cancers." *J HematlOncol*(2013): 6(19): 1756-8722.

13. Wu G, Fang Y, Yang S, Lupton JR, Turner ND. "Glutathione metabolism and its implications for health." *J Nutr* (2004): 134(3): 489-92.

14. Townsend D, Tew K, Tapiero H. "The importance of glutathione in human disease." *Biomed Pharmacother*(2003): 57(3-4): 145-55.

15. Bannai S, Christensen HN, Vadgama JV, et al. "Amino acid transport systems." *Nature* (1984): 311(5984): 308.

16. Meister A. "Glutathione." *Annual Review of Biochemistry* (1983): 52: 711-60.

17. Brieger K, Schiavone S, Miller F, Krause K. “Reactive Oxygen Species: From Health to Disease.” *Swiss Med Wkly*(2012): 142:w13659.

18. Erdamar H, Demirci H, Yaman H. “The effect of hypothyroidism, hyperthyroidism, and their treatment on parameters of oxidative stress and antioxidant status.” *ClinChem Lab Med.* (2008): 46(7): 1004-10.

19. Sanz A, Stefanatos R. “The mitochondrial free radical theory of aging: a critical view.” *Current Aging Sci*(2008): 1(1): 10-21.

20. Hekimi S, Lapointe J, Wen Y. “Taking a ‘good’ look at free radicals in the aging process.” *Trends Cell Biol*(2011): 21(10): 569-76.

21. Waris G, Ahsan H. “Reactive oxygen species: role in the development of cancer and various chronic conditions.” *J Carcinog*(2006): 5: 14.

22. Tabima D, Frizzell S, Gladwin M. “Reactive oxygen and nitrogen species in pulmonary hypertension.” *Free RadicBiol Med* (2012): 52(9): 1970-86.

23. Sorce S, Krause K. “NOX enzymes in the central nervous system: from signaling to disease.” *Antioxid Redox Signal* (2009): 11(10): 2481-504.

24. Block M, Zecca L, Hong J. “Microglia-mediated neurotoxicity: uncovering the molecular mechanisms.” *Nat Rev Neurosci*(2007): 8(1): 57-69.

25. Xu, Jiaquan. "Deaths and Mortality." Centers for Disease Control and Prevention. N.p., 27 Apr. 2016. Web. 1 May 2016. <http://www.cdc.gov/nchs/fastats/deaths.htm>

26. Yan N, Meister A. “Amino acid sequence of rat kidney gamma-glutamylcysteinesynthetase.” *Biochem J* (1997): 328(Pt 1): 99-104.

27. Dalton T, Chen Y, Scott N. “Genetically altered mice to evaluate glutathione homeostasis in health and disease.” *Free RadicBiol and Med* (2004): 37(10): 1511-26.

28. Tu Z, Anders M. “Identification of an important cysteine residue in human glutamate-cysteine ligase catalytic subunit by site-directed mutagenesis.” *Biochem J* (1998): 336(Pt 3): 675-80.

29. Huang C, Anderson M, Meister A. “Amino acid sequence and function of the light subunit of rat kidney gamma-glutamylcysteinesynthetase.” *J BiolChem*(1993): 268: 20578-583.

30. Wild A, Mulcahy R. “Regulation of gamma-glutamylcysteinesynthetase subunit gene expression: insights into transcriptional control of antioxidant defenses.” *Free Radic Res* (2000): 32(4): 281-301.

31. Oppenheimer L, Wellner V, Griffith O, Meister A. “Glutathione synthetase. Purification from rat kidney and mapping of the substrate binding sites.” *J BiolChem*(1979): 254(12): 5184-90.

32. Grant C, MacIver F, Dawes I. “Glutathione synthetase is dispensable for growth under both normal and oxidative stress conditions in the yeast Saccharomyces cerevisiae due to an accumulation of the dipeptide gamma-glutamylcysteine.” *MolBiol Cell* (1997): 8(9): 1699-1707.

33. Lu S. “Regulation of hepatic glutathione synthesis: Current concept and controversies.” *FASEB J* (1999): 13(10): 1169-83.

34. Bannai S, Tateishi N. “Role of membrane transport in metabolism and function of glutathione in mammals.” *J Membrane Biol*(1986): 89(1): 1-8.

35. Lu SC, Ge J, Kuhlenkamp J. “Insulin and glucocorticoid dependence of hepatic gamma-glutamylcysteinesynthetase and GSH synthesis in the rat: Studies in cultured hepatocytes and in vivo.” *J Clin Invest* (1992): 90(2): 524-32.

36. Cai J, Sun WM, Lu SC. “Hormonal and cell density regulation of hepatic gamma-glutamylcysteinesynthetase gene expression.” *MolPharmacol*(1995): 48:212-18

37. Fu Y, Zhou YJ, Lu SC. “Epigallocatechin-3-gallate inhibits growth of activated hepatic stellate cells by enhancing the capacity of glutathione synthesis.” *MolPharmacol*(2008): 73: 1465-73.

38. Lee J, Kang J, Stipanuk M. “Differential regulation of glutamate-cysteine ligase subunit expression and increased holoenzyme formation in response to cysteine deprivation.” *Biochem J* (2006): 393(Pt 1): 181-90.

39. Reed M, Thomas R, Pavisic J. “A mathematical model of glutathione metabolism.” *TheorBiol and Med Mod* (2008): 5(1):8.

40. Halprin, K. “The measurement of Glutathione in Human Epidermis using Glutathione Reductase.” *J InvestigDerm*(1967): 48(2): 149-52.

41. Mendoza-Cozatl D, Moreno-Sanchez R. “Control of glutathione and phytochelatin synthesis under cadmium stress. Pathway modeling for plants.” *J TheorBiol*(2006): 238: 919-36.

42. Ookhtens M, Mittur A, Erhart N. “Changes in plasma glutathione concentrations, turnover, and disposal in developing rats.” *Amer J Physiol*(1994): 266(3): 979-88.

44. "All living systems require constant input of free enery and organisms capture and store free energy for use in biological processes." Julia's Blog. N.p., 06 Oct. 2014. Web. 21 May 2016. <http://sites.saschina.org/juliapx2016/2014/10/06>

45. "Electron Transport Chain." Science in a Can. N.p., 19 Jul. 2014. Web. 21 May 2016. <http://sciencesoup.tumblr.com/post/92192632459/>

46. Lu S. “Regulation of Glutathione Synthesis.” *Mol Aspects Med* (2010): 42-59.

47. Kowan K, Batist G, Tulpule A. “Similar biochemical changes associated with multidrug resistance in human breast cancer cells and carcinogen-induced resistance to xenobiotics in rats.” *Proc Nat Acad of Sci of USA.* (1986): 83(24): 9328-32.

48. Mattill HA. "Antioxidants." *Annual Review of Biochemistry* (1947) **16**: 177–92.

APPENDICES

Appendix A

Model Equations

A.1 Rates and Equations for Model

BLOOD COMPARTMENT RATES:

$$V_{b,GSSG\rightarrow aa} = (2)(67.5)[GSSG_B]$$

$$V_{b,GSH\rightarrow aa} = (90)[GSH_B]$$

$$V_{b,cys,metabolism} = (0.1)(0.25)[cys_B]$$

$$V_{b,glu,metabolism} = (0.1)[glu_B]$$

$$V_{b,gly,metabolism} = (0.1)[gly_B]$$

$$V_{b,GSSG,metabolism} = (7.5)[GSSG_B]$$

$$V_{b,GSH,metabolism} = (0.7)[GSH_B]$$

TRANSMEMBRANE RATES:

$$V_{gly,in} = \frac{V_m[gly_B]}{(K_m + [gly_B]) - (K_o[gly_C])}$$

$$V_{glu,in} = \frac{V_m[glu_B]}{(K_m + [glu_B]) - (K_o[glu_C])}$$

$$V_{cys,in} = \frac{V_{\max}[cys_B]}{K_m + [cys_B]}\left(\frac{(k_4 + k_5)[GSH_{ss}]^2}{[GSH_{ss}]^2 k_4 + [GSH_C]^2 k_5}\right)$$

$$V_{mBBr\rightarrow cell} = \frac{V_{\max}[mBBr_B]}{K_m + [mBBr_B] - K_o[mBBr_C - mBBr_B]}$$

$$V_{GSH\rightarrow blood} = \frac{V_{\max,H}[GSH_C]}{K_{m,H}+[GSH_C]} + \frac{V_{\max,L}[GSH_C]^3}{K_{m,L}{}^3+[GSH_C]^3}$$

$$V_{GSSG\rightarrow blood} = \frac{V_{\max,H}[GSSG_C]}{(K_{m,H}+[GSSG_C])\frac{K_H+[H_2O_2]}{K_H+[ssH_2O_2]}} + \frac{V_{\max,L}[GSSG_C]}{(K_{m,L}+[GSSG_C])\frac{K_L+[H_2O_2]}{K_L+[ssH_2O_2]}}$$

$$V_{GSBi\rightarrow blood} = \frac{V_{\max}[GSBi_C]}{K_m+[GSBi_C]-K_e[GSBi_B]}$$

CELL COMPARTMENT RATES:

$$V_{c,mBBr,metabolism} = (0.01)[mBBr_c]$$

$$V_{c,GSBi,metabolism} = (0.003)[GSBi_c]$$

$$V_{c,GSH,metabolism} = (0.002)[GSH_c]$$

$$V_{c,GSSG,metabolism} = (0.1)[GSSG_c]$$

$$V_{c,glu,metabolism} = (0.07)[glu_c]$$

$$V_{c,cys,metabolism} = (0.35)\frac{[cys_c]^2}{200}$$

$$V_{GCL} = \frac{V_{\max}([glu_C][cys_C]-\frac{[GluCys]}{K_e})}{K_{m,cys}K_{m,glu}+K_{m,cys}[glu_C]+K_{m,glu}[cys_C](1+\frac{[GSH_C]}{K_i}+\frac{[glu_C]}{K_{m,glu}})+\frac{[GluCys]}{K_p}+\frac{[GSH_C]}{K_i})} * \frac{K_a+[ssH_2O_2]}{K_a+[H_2O_2]} * \frac{K_b+[mBBr_C]}{K_b}$$

$$V_{GS} = \frac{V_{\max}([gly_C][GluCys] - \frac{[GSH_C]}{K_e}}{K_{m,GluCys}K_{m,gly} + K_{m,gly}[GluCys] + K_{m,GluCys}[gly_c](1 + \frac{[GluCys]}{K_{m,GluCys}}) + \frac{[GSH_C]}{K_p}}$$

$$V_{GST} = \frac{V_{\max}[GSH_C][mBBr_C]}{k_1 k_2 + k_2[GSH_C] + k_1[mBBr_C] + [GSH_C][mBBr_C]}$$

$$V_{GPX} = (2)V_{max}\frac{[GSH_c]}{(K_{mg} + [GSH_c])^2}\frac{[H_2O_2]}{(9)[ssH_2O_2] + [H_2O_2]}$$

$$V_{GR} = \frac{(2)V_{max}\frac{[GSSG_c]}{K_{m,1}}\frac{[NADPH]}{K_{m,2}}}{1 + \frac{[GSSG_c]}{K_{m,1}} + \frac{[NADPH]}{K_{m,2}} + \frac{[GSSG_c]}{K_{m,1}}\frac{[NADPH]}{K_{m,2}}}$$

Appendix B

ParameterValues

B.1 Initial Conditions

Substrate	**Cell Concentration (µM)**	**Blood Concentration (µM)**
cysteine	195.0	186.0 (constant)
glutamate	3219.0	60.4 (constant)
glycine	924.0	221.0 (constant)
GluCys	9.8	N/A
GSH	6581.0	12.7
GSSG	61.3	0.0
GSBi	0.0	0.0
mBBr	0.0	5500.0
H_2O_2	0.01 (constant)	N/A
ssH_2O_2	0.01 (constant)	N/A
NADPH	50.0 (constant)	N/A

B.2 Equation Constants (µM/hr, µM)

$V_{cys,in}$	V_{max}=14950, 16500 K_m=2100 k_4 = 0.5, 2.5 k_5 = 2, 50 GSH_{ss} = 4700, 5200
$V_{glut,in}$	V_{max}=28000 K_m=300

	K_o=1
$V_{gly,in}$	V_{max}=4600 K_m=150 K_o=1
$V_{mBBr \rightarrow cell}$	V_{max}=25000 K_m=800 K_o=0.01
V_{GCL}	V_{max}=3600, 4500 K_a=0.01 $K_{m,glu}$=1900 $K_{m,cys}$=100 K_i=8200 K_p=300 K_e=5597 K_b=300
V_{GS}	V_{max}=5400 $K_{m,glucys}$=22 $K_{m,gly}$=300 K_p=30 K_e=5600
V_{GST}	V_{max}=8950, 16900 k_1=200 k_2=200
$V_{GSSG \rightarrow blood}$	$V_{max,H}$=40 $k_{m,H}$=1250 k_H=0.05 $V_{max,L}$=4025 $k_{m,L}$=7100 k_L=0.05
$V_{GSH \rightarrow blood}$	$V_{max,H}$=150 $K_{m,H}$=150 $V_{max,L}$=1100 $K_{m,L}$=3000
$V_{GSBi \rightarrow blood}$	V_{max}=2000, 3500 K_e=1250

	K_m=500, 3900
V_{GPX}	V_{max}=4500 K_{mg}=1330
V_{GR}	V_{max}=892.5 K_{m1}=107 K_{m2}=10.4

Appendix C

Matlab Code

C.1 Code for Normalizing and Plotting Data

```
%normalize results
GSHnorm=x(1:end,1)/max(x(1:end,1));
GSBinorm=x(1:end,3)/max(x(1:end,3));
mBBrnorm=x(1:end,2)/max(x(1:end,2));

%import Data
[GSH2]=xlsread('GSH2ToImport.xlsx');
[GSBi2]=xlsread('GSBi2ToImport.xlsx');
[GSH]=xlsread('GSH1ToImport.xlsx');
[GSBi]=xlsread('GSBi1ToImport.xlsx');
[DMSO]=xlsread('DMSO1ToImport.xlsx');

DataT=[17.02:0.02:21.00];
mBBr=zeros(length(DataT),1);
mBBr(1:end)=mBBrnorm(1:length(mBBr));

GSBiAverageMatrix=[GSBi,GSBi2];
GSBiAverage=mean(GSBiAverageMatrix,2);
GSBiAverageNorm=GSBiAverage(1:end)/max(GSBiAverage);
GSHAverageMatrix=[GSH,GSH2];
GSHAverage=mean(GSHAverageMatrix,2);
GSHAverageNorm=GSHAverage(1:end)/max(GSHAverage);

%shift model timescale to match data
tshift=t;
tdelt=17.0;
 for i=1:length(tshift)
tshift(i)=tshift(i)+tdelt;
 end

GSHResidAvg=GSHAverageNorm-GSHnorm(5:4+length(GSH));
GSBiResidAvg=GSBiAverageNorm-GSBinorm(5:4+length(GSBi));
  %GSHResidAvg=GSHAverageNorm(5:4+length(GSHnorm))-GSHnorm;
  %GSBiResidAvg=GSBiAverageNorm(5:4+length(GSBinorm))-GSBinorm;

figure
```

```
hold on
ylim([0,1]);
xlim([tdelt,22]);
scatter(DataT,DMSO,'+');
plot(DataT,mBBr,'c');
title('Normalized DMSO measurements plotted with modeled cellular Bromobimane (mBBr)
concentration')
ylabel('Normalized Concentration')
xlabel('Time (h)');
legend('DMSO','mBBr');
hold off

figure
hold on
ylim([0,1]);
xlim([tdelt,22]);
scatter(DataT,GSH,'+');
scatter(DataT,GSBi,'+','r');
plot(tshift,GSHnorm,'g');
plot(tshift,GSBinorm,'m');
title('NormalizedGlutathione (GSH) and Glutathione-bimane (GSBi) response to
Bromobimaneexposure (mBBr) dataset 1')
ylabel('Normalized Concentration');
xlabel('Time (h)');
legend('GSH data', 'GSBidata','GSH model', 'GSBi model');
hold off

figure
hold on
ylim([0,1]);
xlim([tdelt,22]);
scatter(DataT,GSH2,'+');
scatter(DataT,GSBi2,'+','r');
plot(tshift,GSHnorm,'g');
plot(tshift,GSBinorm,'m');
title('NormalizedGlutathione (GSH) and Glutathione-bimane (GSBi) response to
Bromobimaneexposure (mBBr) dataset 2')
ylabel('Normalized Concentration')
xlabel('Time (h)')
legend('GSH data 2', 'GSBidata','GSH model', 'GSBi model')
hold off
```

```
figure
hold on
ylim([0,1]);
xlim([tdelt,22]);
scatter(DataT,GSHAverageNorm,'+');
scatter(DataT,GSBiAverageNorm,'+','r');
plot(tshift,GSHnorm,'g');
plot(tshift,GSBinorm,'m');
%plot(tshift,BrBinorm,'c');
title('NormalizedGlutathione (GSH) and Glutathione-bimane (GSBi) response to
Bromobimaneexposure (mBBr); Averaged Data')
ylabel('Normalized Concentration')
xlabel('Time (h)')
legend('GSH Average', 'GSBiAverage','GSH model', 'GSBi model')
hold off

figure
subplot(2,1,1)
hold on
scatter(GSH,GSHResidAvg);
plot(xlim,[0 0],'k-')
hold off
title('Residual vs GSH data from averaged experimental results')
xlabel('GSH')
ylabel('Residual')
subplot(2,1,2)
hold on
scatter(GSBi,GSBiResidAvg);
plot(xlim,[0 0],'k-')
hold off
title('Residual vsGSBi data from averaged experimental results')
xlabel('GSBi')
ylabel('Residual')

totdiffGSH=zeros(1,length(GSH));
totdiffGSBi=zeros(1,length(GSBi));

for i=1:length(GSH)
totdiffGSH(i)=(GSH(i)-(sum(GSH)/length(GSH)))^2;
totdiffGSBi(i)=(GSH(i)-(sum(GSBi)/length(GSBi)))^2;
resdiffGSH(i)=(GSH(i)-GSHnorm(i+4))^2;
resdiffGSBi(i)=(GSBi(i)-GSBinorm(i+4))^2;
```

```
end

GSHSStot=sum(totdiffGSH);
GSBiSStot=sum(totdiffGSBi);
GSHSSres=sum(resdiffGSH);
GSBiSSres=sum(resdiffGSBi);

RsquareGSH=1-(GSHSSres/GSHSStot);
RsquareGSBi=1-(GSBiSSres/GSBiSStot);
```

Appendix D

Supplemental Graphs

D.1 Cellular Concentration of Other Substrates

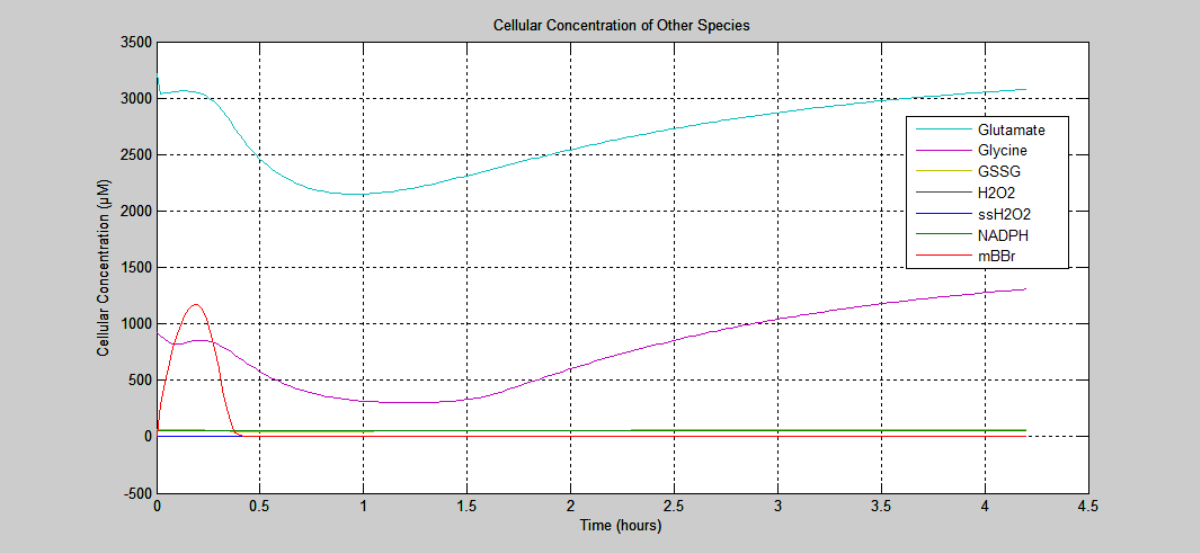

Figure D.1. Cellular Concentration of Other Substrates. Other species mentioned but not shown in the body of the paper are graphed here. Here, t=0 corresponds to the experimental time of t=17 hours when mBBr dosage occurred.